AGU ADVANCING EARTH AND SPACE SCIENCES

Water Resources Research

RESEARCH ARTICLE
10.1029/2026WR044233

Compound Impacts of Drought and Soil Salinity on Maize Productivity

Huiying Li[1] and **Shuo Wang**[1,2]

[1]State Key Laboratory of Climate Resilience for Coastal Cities, Department of Land Surveying and Geo-Informatics, The Hong Kong Polytechnic University, Hong Kong, China, [2]Otto Poon Research Institute for Climate-Resilient Infrastructure and Research Institute for Land and Space, The Hong Kong Polytechnic University, Hong Kong, China

Key Points:

- More frequent drought days are associated with significant declines in maize yield
- The combined effects of drought and soil salinity lead to greater maize yield losses than drought alone, with salinity contributing an additional loss of over 5%
- Improper irrigation practices may be associated with increased soil salinization and undermine efforts to mitigate drought

Supporting Information:

Supporting Information may be found in the online version of this article.

Correspondence to:

S. Wang,
shuo.s.wang@polyu.edu.hk

Citation:

Li, H., & Wang, S. (2026). Compound impacts of drought and soil salinity on maize productivity. *Water Resources Research*, *62*, e2026WR044233. https://doi.org/10.1029/2026WR044233

Received 30 MAR 2026
Accepted 2 AUG 2026

Author Contributions:

Conceptualization: Shuo Wang
Data curation: Huiying Li
Formal analysis: Huiying Li, Shuo Wang
Funding acquisition: Shuo Wang
Investigation: Shuo Wang
Methodology: Huiying Li, Shuo Wang
Project administration: Shuo Wang
Resources: Shuo Wang
Software: Huiying Li
Supervision: Shuo Wang
Validation: Huiying Li, Shuo Wang
Visualization: Huiying Li
Writing – original draft: Huiying Li
Writing – review & editing: Shuo Wang

Abstract Intensifying soil drought poses a significant threat to maize yields in China. However, the compounding effects of soil drought and salinity remain poorly understood. Here, we analyze maize yield trends in China from 1982 to 2016 and show that an increase in the total number of drought days is associated with significant yield declines. We find that the co-occurrence of drought and soil salinity (CODS) amplifies maize yield-loss risk, with the probability of yield loss exceeding 20% and remaining higher than under drought alone. Compared with drought-only conditions, CODS increases the additional yield-loss risk by approximately five percentage points. These findings are further supported by analyses in the North China Plain and the Songnen Plain, where irrigated areas exhibit more negative yield anomalies than rain-fed areas under comparable drought conditions, suggesting that irrigation practices may be associated with increased soil salinity and thereby reduce the effectiveness of drought mitigation. This study underscores the urgent need for integrated soil and water management strategies that simultaneously address drought resilience and salinity control to safeguard China's maize production.

Plain Language Summary Climate change is increasing the frequency and severity of droughts, threatening maize production in China. Our study finds that maize yields decline as the number of drought days increases, and this damage is amplified when drought occurs in combination with soil salinity. This interaction creates a higher risk of yield loss than drought alone, with soil salinity resulting in additional yield-loss risk of more than 5%. We validate this finding in the North China Plain and the Songnen Plain, where irrigated areas exhibit more negative yield anomalies than rain-fed areas under comparable drought conditions, suggesting that irrigation-associated salinity may reduce the effectiveness of drought mitigation. These results highlight the urgent need for improved soil and water management to protect maize production under climate change.

1. Introduction

The increasing frequency and intensity of extreme climate events pose significant challenges to agricultural production (Gebrechorkos et al., 2025; Zhou et al., 2023). Among these, drought is a predominant abiotic stressor (Hultgren et al., 2025), affecting 40% of global irrigated areas (The State of Food Security and Nutrition in the World 2020, 2020). Drought is characterized not only by substantial reductions in precipitation over extended periods but also by variations in its frequency, duration, and spatial distribution, all of which threaten the stability of agricultural systems (Chen et al., 2026; Gebrechorkos et al., 2025; Tang et al., 2025; Zhang et al., 2024). Biologically, drought stress reduces key morphological and physiological traits, including photosynthetic capacity, leaf water potential, sap flow, and stomatal conductance (Bhusal et al., 2019). In recent years, many countries have experienced substantial declines in crop yields due to drought events (Freedman et al., 2025; Hultgren et al., 2025). As a major agricultural country, China is no exception, with several regions reporting notable yield losses directly attributed to drought stress (Li et al., 2024; F. Xu et al., 2024). According to data from the Bulletin of Food and Drought Disasters in China, the country suffers annual drought-related agricultural losses of 16.302 billion kilograms between 1950 and 2016, accounting for more than 60% of total grain losses caused by natural disasters (Zhang et al., 2019).

Maize plays a critical role in China's agricultural production and food security (National Bureau of Statistics of China, 2024). Owing to its high water demand and sensitivity, maize is particularly vulnerable to water deficits (Challinor et al., 2014; Daryanto et al., 2016). Irrigation is therefore an important management response for reducing drought-induced yield losses. Previous modeling-based studies have shown that irrigation can partly mitigate the negative effects of drought on crop productivity, particularly when irrigated systems are compared with rainfed systems (Deb et al., 2022). However, the drought-mitigation benefit of irrigation may not eliminate potential salinity-related risks when irrigation water quality or salt leaching is not properly managed. In addition to drought, maize is also susceptible to salinity stress (Rhoades et al., 1992; Tanji et al., 2002). Excessive soil salt imposes ionic toxicity on plant roots and disrupts cellular osmotic balance, thereby reducing stomatal conductance. This limitation in gas exchange inhibits CO_2 uptake and ultimately diminishes the rate of photosynthesis (Ouyang et al., 2017). Although maize is generally avoided on highly saline soils, both natural and anthropogenic processes can cause soil salinity to accumulate to stress-inducing levels. Natural mechanisms, such as evaporation, can transport saline groundwater to the soil surface via capillary force (Abrol et al., 1988; Corwin, 2021; LI, 2025). Similarly, improper irrigation practices, saline water irrigation, and fertilization directly or indirectly contribute to soil salt accumulation (Corwin, 2021; Singh, 2015; Utset & Borroto, 2001). Currently, 17 countries worldwide, including China, use saline water for irrigation (Hussain et al., 2020). Although generally less suitable for agriculture than freshwater, saline water remains a major irrigation water source in many arid regions, particularly in developing countries where freshwater scarcity and growing population intensify demand (Hagage et al., 2024; Soni et al., 2021). Soil salinity increases with the concentration of applied saline irrigation water (Soni et al., 2021). As soil water evaporates, salts accumulate in the soil solution, resulting in simultaneous drought and salinity stress (Hailu & Mehari, 2021). These local physiological and soil-process mechanisms can accumulate into spatially heterogeneous salinity patterns across agricultural regions. Existing research indicates that the electrical conductivity of soil extract (EC_e) is commonly used to quantify soil salinity levels (Corwin, 2021). Therefore, gridded ECe data provide a useful basis for evaluating whether areas with elevated soil salinity experience greater maize yield losses under drought conditions at large spatial scales.

Most plants are affected by either drought or salinity; in many cases, these stressors co-occur in arid and semi-arid regions (Sahin et al., 2018). While numerous studies have examined the individual effects of drought or salinity on maize performance (Angon et al., 2022; Bhusal et al., 2019; Daryanto et al., 2016; Lobell et al., 2014; Ouyang et al., 2017), the combined impact remains challenging to assess due to its complexity (Mehrabi et al., 2022; Wen et al., 2023). In particular, quantitative assessment of growth reduction under combined drought and salinity stress, compared to individual drought, has been insufficiently reported (Ibrahim et al., 2019; Ni et al., 2024; Sahin et al., 2018). This leaves a gap in understanding the synergistic risks these factors pose to crop yield. Previous studies indicate that soil moisture often exerts a stronger influence on crop yield than salinity (Du et al., 2023; Sahin et al., 2018). Based on this understanding, this study treats soil drought as the primary factor affecting maize yield, with salinity as a secondary factor, to investigate yield responses to their combined effects. From a risk management perspective, this study explores whether increasing soil salinity significantly heightens the risk of maize yield loss under intensifying drought conditions.

In this study, we examine the long-term trend of maize yield changes across China from 1982 to 2016 against the backdrop of intensifying drought conditions. We further assess the potential impacts of individual drought events and the co-occurrence of drought and soil salinity (CODS) on maize yields during the maize-growing season. In addition, we identify the dominant climatic factors driving maize yield anomalies. Considering the unique salt stress and saline irrigation practices in the North China Plain and the Songnen Plain, we further investigate the impacts of human activities in these two regions. Our findings highlight the significant risk posed by CODS to maize yield and provide valuable insights into the consequences of inappropriate irrigation practices, such as the use of saline water. This study aims to furnish scientific evidence to support agricultural management and effective emergency response planning.

2. Methods

2.1. Data Set

In this study, the Crop Calendar data set was used to provide planting and harvesting dates for maize cultivation at a 0.5° spatial resolution (Sacks et al., 2010). The Global Data set of Historical Yields (GDHY) was used to investigate the maize yield trend, which offers gridded maize yield data for major and secondary maize crops from 1981 to 2016 at a 0.5° resolution (Iizumi & Sakai, 2020). For validation, we used the GlobalCropYield5min data set, resampled to 0.1°, which provides maize yield data from 1982 to 2015 (Cao et al., 2025).

Daily soil moisture (SM) data were obtained from the European Center for Medium-Range Weather Forecasts (ERA5) (Hersbach et al., 2020). We used the top two soil layers, which represent shallow soil moisture conditions

10.1029/2026WR044233

and are relevant to near-surface water availability during maize growth. However, these layers do not fully capture the entire maize root zone, because maize roots can extend deeper than the upper soil layers depending on soil properties and growth stage. Therefore, ERA5 top-layer SM is interpreted here as a spatially consistent indicator of shallow soil drought conditions rather than a complete measure of root-zone water availability. We also used the Global Land Evaporation Amsterdam Model (GLEAM) data set (Miralles et al., 2025) as an independent validation data set represents soil moisture over the 0–100 cm layer. Both data sets were resampled to a $0.5° \times 0.5°$ resolution.

The electrical conductivity of soil extract (EC_e) is used to quantify soil salinity levels (Corwin, 2021). We obtained the yearly surface EC_e data for 1980–2018 from the University of Manchester (Hassani et al., 2020), which was developed using machine learning techniques and remote sensing. This data set focuses on the topsoil layer (0–30 cm) and covers latitudes from 55°S to 55°N, including tropical, subtropical, and temperate zones, while excluding water bodies, permanent wetlands, urban and built-up areas, as well as permanent snow and ice. The EC_e data were resampled to 0.5° to match the maize yield data. Although topsoil salinity is relevant to seedling establishment, near-surface root activity, and salt accumulation caused by evaporation and capillary rise, annual 0–30 cm EC_e may not fully capture growing-season salinity dynamics or deeper root-zone salinity stress. Therefore, we interpret this data set as a long-term surface salinity indicator suitable for large-scale spatial analysis, while acknowledging that depth-specific and seasonally resolved salinity data would better represent crop salinity stress.

Climatic data were derived from the gridded Climate Research Unit Time Series (CRU TS v.4.04) global data set, with a spatial resolution of 0.5° (Harris et al., 2020). Vapor pressure deficit (VPD) was calculated as the difference between saturated water vapor pressure (SVP) and actual water vapor pressure (VAP). Temperature (T), potential evapotranspiration (PET), and precipitation (P) data were also obtained from the CRU TS data set.

2.2. Maize Yield Anomaly

The relative yield anomaly (y_t) for each grid cell, calculated as the difference between actual yield (y_t) and expected yield (U_t) divided by the expected yield (U_t), is given as:

$$y_t = \frac{Y_t - U_t}{U_t}, \tag{1}$$

where y_t is the maize yield value (tons per hectare, t·ha^{-1}) and U_t is the expected yield value (t·ha^{-1}) at year t U_t is estimated based on centered 7-year moving window mean value (Troy et al., 2015), including the focal year, the previous 3 years, and the following 3 years. For endpoint years, the window was shortened according to data availability. This moving-window approach allows us to reduce the influence of long-term yield trends related to technological advances, seed improvement, rising CO_2, policy changes, and other non-climatic influences, but it should not be interpreted as fully isolating climate effects. The yield loss is defined as relative yield anomalies below −10% of the expected yields ($y_t < -0.1$) (Ben-Ari et al., 2018).

2.3. Definition of Yield Loss Risk

The copula-based model was used to estimate the potential impacts of individual drought and CODS on maize yields during the maize-growing season, defined as the period from planting start to harvest start. Copulas effectively capture extreme events, such as droughts and floods, by modeling the tails of the distribution (Chen & Wang, 2023; Zhang et al., 2022).

Here, we considered five commonly used bivariate copula families (Gaussian, Student-t, Clayton, Gumbel, and Frank) to fit the joint probability distribution of the total number of drought days (TNDD) for individual drought (d), the TNDD of the CODS(s), and the relative yield anomaly (y).

$$\rho_{d,y}(d,y) = \rho_d(d) \cdot \rho_y(y) \cdot C(d,y,\theta_{d,y}), \tag{2}$$

$$\rho_{d,s,y}(d,s,y) = \rho_d(d) \cdot \rho_s(s) \cdot \rho_y(y) \cdot C(d,s,\theta_{d,s}) \cdot C(d,y,\theta_{d,y}) \cdot C(h(s,d,\theta_{d,s}), h(y,d,\theta_{d,y})\theta_{s,y|d}), \tag{3}$$

10.1029/2026WR044233

where $\rho_d\ (d)$, $\rho_s\ (s)$, and $\rho_y\ (y)$ are marginal distributions. C is the copula density. θ is copula parameters. The h-function is the conditional probability distribution function.

The conditional cumulative probability $P(.|.)$ is determined using the canonical vine (C-vine) and the drawable vine (D-vine) structures (Chen & Wang, 2023; Zhang et al., 2022). Moreover, the maximum Likelihood Estimation (MLE) method was used to fit marginal distributions and estimate the copula parameters, using Gamma distributions for salinity and TNDD, and a normal distribution for yield anomaly. The Bayesian Information Criterion (BIC) was used to select the appropriate vine structure (Dißmann et al., 2013). After determining the vine structure, conditional probabilities, including $P\left(y < y_1/d > d_1, s \geq s_1\right)$ and $P\left(y < y_1/d > d_1\right)$, were computed analytically using the cumulative distribution functions (CDFs) of bivariate copulas.

The choice of marginal distributions was based on the empirical characteristics of the variables. EC_e and TNDD are non-negative variables and exhibit right-skewed distributions with long tails. Therefore, Gamma distributions provided a reasonable approximation of their marginal distributions and were therefore adopted in the copula analysis. In contrast, relative yield anomaly is a continuous variable centered around zero and shows an approximately symmetric distribution after detrending, supporting the use of a normal distribution. The empirical distributions supporting these choices are shown in Figure S8 of Supporting Information S1.

The conditional CDF of yield loss under CODS and individual drought can be expressed as:

$$P\left(y < y_1/d > d_1\right) = \frac{\partial C_{d,y}\left(P\left(y < y_1/d\right), P(d > d_1)\right)}{\partial P(d > d_1)} = h\left[h\left(y < y_1, d, \theta_{d,y}\right), h(d > d_1, \theta_d), \theta_{y|d}\right], \tag{4}$$

$$P\left(y < y_1/d > d_1, s \geq s_1\right) = \frac{\partial C_{d,s,y}\left(P\left(y < y_1/d, s\right), P(d > d_1), P(s \geq s_1)\right)}{\partial P(d > d_1) \partial P(s \geq s_1)}$$
$$= h\left[h\left(y < y_1, d, s, \theta_{d,y}, \theta_{s,y|d}\right), h(d > d_1, \theta_d), h(s > s_1, \theta_s), \theta_{y|d,s}\right], \tag{5}$$

where $y_1 = -0.1$, represents the yield loss. $d_1 = 0$, represents non-drought, $d > d_1$ represents drought. $s_1 = 2$, represents the threshold of saline soil, $s \geq s_1$ represents saline soil. $P\left(y < y_1/d > d_1\right)$ calculates the conditional probabilities of yield loss under individual drought. $P\left(y < y_1/d > d_1, s \geq s_1\right)$ calculates the conditional probabilities of yield loss under the co-occurrence of drought and soil salinity (CODS).

Equations 6 and 7 can be used to estimate the risk of yield loss caused by individual drought and CODS based on probabilistic model simulations:

$$\hat{y} = f(d, \tau) = P_y^{-1}\left\{h^{-1}\left(h^{-1}\left(\tau | h(P_y(y) | P_d(d), \theta_{d,y}), \theta_{y|d}\right) | P_d(d), \theta_{d,y}\right)\right\}, \tau \in (0, 1), \tag{6}$$

$$\hat{y} = f(d, s, \tau) = P_y^{-1}\left\{h^{-1}\left(h^{-1}\left(\tau | h(P_s(s) | P_d(d), \theta_{d,s}), \theta_{s,y|d}\right) | P_d(d), \theta_{d,y}\right)\right\}, \tau \in (0, 1), \tag{7}$$

where τ indicates random probability levels (e.g., $\tau = 0.01, 0.1, \ldots, 0.9$); P indicates cumulative marginal distribution functions. To improve the stability of the estimated conditional yield-loss risk, we used Monte Carlo simulations to generate multiple (e.g., 500) samples of τ from the uniform distribution U (0,1). These simulations were used to evaluate yield-loss risk across probability levels after the copula structure and parameters had been fitted. Therefore, they should be interpreted as Monte Carlo sampling of conditional probability levels rather than as sampling of copula-parameter uncertainty.

2.4. XGBoost and SHAP

XGBoost is a gradient-boosted machines and an ensemble learning model (Chen & Guestrin, 2016) that iteratively integrates multiple weak predictive models into a robust unified model (Bentéjac et al., 2021). It is well suited for probability estimation under nonlinear responses, thresholds, and feature interactions. In this study, we applied a logistic binary risk discrimination of crop yield loss events. The model superimposes regression trees in an additive manner and minimizes the logistic loss with structural regularization. During the training process, the second-order Taylor approximation is used to obtain the optimal weights and split gains of leaf nodes, which determine the best partitioning and control the structural complexity of the model.

$$\hat{z}_i = \sum\nolimits_{t=1}^{T} f_t(x_i), \tag{8}$$

$$\hat{p}_i = \sigma(\hat{z}_i) = \frac{1}{1 + e^{-\hat{z}_i}}, \tag{9}$$

where x_i denotes the feature vector of sample i containing predictors including P, PET, VPD, T, SM, and EC_e. Each $f_t(\cdot)$ corresponds to a regression tree in the ensemble, T is the total number of trees ($T = 350$). $\sigma(\cdot)$ is the sigmoid link function that converts the model margin $\hat{z}_i$ (log-odds) into the probability of event occurrence $\hat{p}_i$.

The model minimizes a regularized logistic loss:

$$L = \sum\nolimits_{i=1}^{\mathrm{n}} \left[-y_i \log(\hat{p}_i) - (1 - y_i)\log(1 - \hat{p}_i)\right] + \gamma T + \frac{1}{2}\lambda \sum\nolimits_{j=1}^{T} \omega_j^2, \tag{10}$$

where $y_i \in \{0, 1\}$ denotes yield no loss or loss; n is the number of training samples; γ controls the penalty for the number of leaves T in a tree; λ is the L2 regularization coefficient that constrains the magnitude of leaf weights ω_j, and ω_j is the prediction score assigned to leaf node j.

SHAP (Shapley Additive exPlanations) provides additive, sign-consistent attributions that decompose each prediction relative to the model expectation, and extends to pairwise interaction attributions, which enabling local explanations that can be aggregated into global structures (Lundberg & Lee, 2017). For tree ensembles, SHAP ensures consistency and local accuracy, with stable attributions across tasks; interaction SHAP isolates pairwise effects (Lundberg et al., 2020).

$$f(x) = \mathrm{E}[f(x)] + \sum\nolimits_{i=1}^{p} \phi_i(x), \tag{11}$$

where $f\ (x)$ represents the model output for instance x; $\mathrm{E}[f\ (X)]$ is the expected prediction across a background distribution; p is the number of input features; $\varnothing_i\ (x)$ denotes the Shapley value for feature i, corresponding to its marginal contribution to the prediction of x.

Each Shapley value is defined as:

$$\phi_i(x) = \sum\nolimits_{S \subseteq F \setminus \{i\}} \frac{|S|!(p - |S|) - 1!}{p!} [v(S \cup \{K\}) - v(S)], \tag{12}$$

where F denotes the set of all features. S is a subset of features excluding i. $v(S)$ represents the expected model output when only the features in S are known. The expression inside the brackets represents the marginal contribution of feature i.

It should be noted that SHAP values provide model-based explanations of predictor contributions to the trained XGBoost model, rather than causal evidence. Therefore, in this study, SHAP analysis is used to identify the relative importance and directional associations of environmental predictors with maize yield-loss risk, but not to infer causal relationships among drought, salinity, and yield loss. This interpretation is consistent with recent hydroclimatic studies that have used SHAP and interpretable machine learning to identify dominant drivers or controls of floods and drought-related processes, rather than as standalone causal attribution tools (Ghaneei et al., 2026; Xu et al., 2024).

2.5. Definition of Dryness Conditions and Drought Events

We defined soil drought as occurring when soil moisture (SM) percentiles fall below a threshold value continuously over time and across a contiguous area (Andreadis & Lettenmaier, 2006), reflecting the rarity and extremity of the event. In this study, a threshold value of the 20th percentile of SM quantile was used to distinguish drought from non-drought, following previous drought identification work (Andreadis & Lettenmaier, 2006; Wang et al., 2008). This is also the threshold used in the U.S. Drought Monitor (available at https://droughtmonitor.unl.edu/About/AbouttheData/DroughtClassification.aspx).

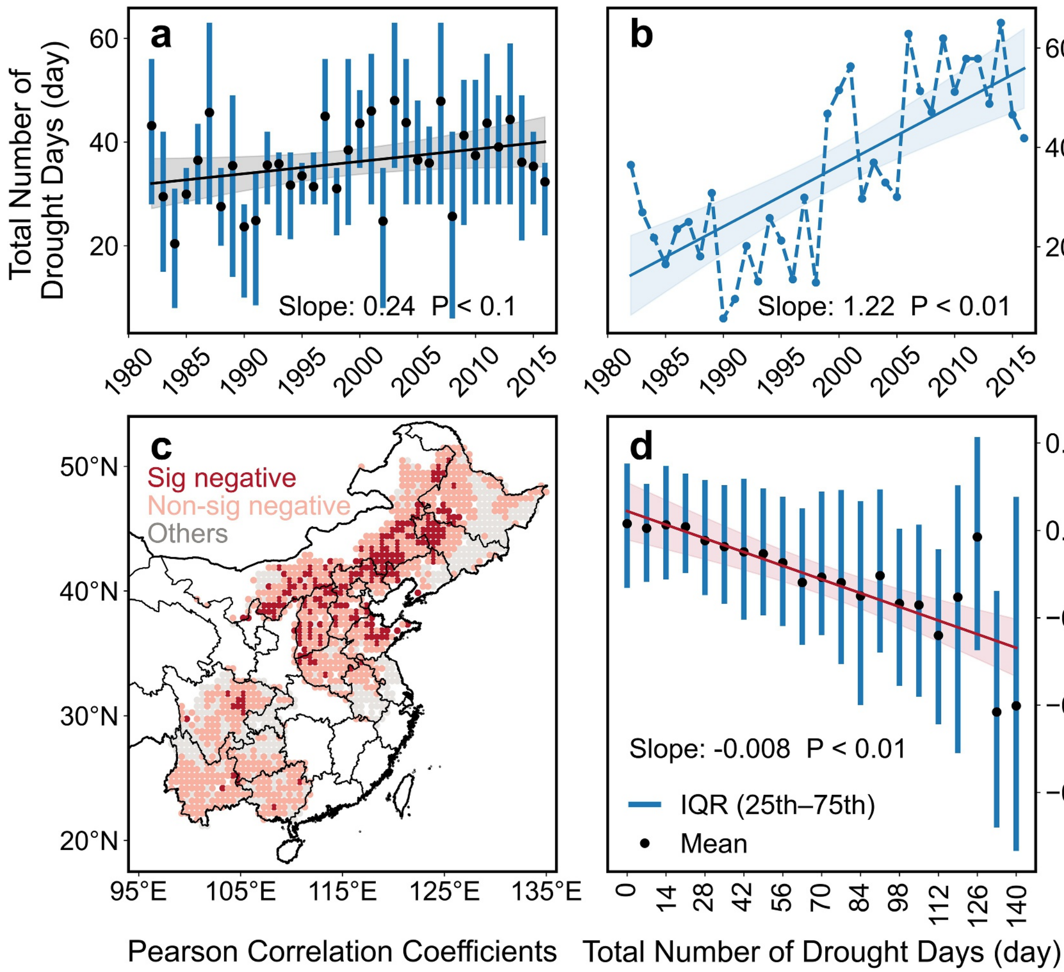

Figure 1. Drought trends and the correlation between drought and yield. (a) Temporal trend in the total number of soil drought days from 1982 to 2016. The black dot represents the mean value, and the blue solid line represents the 25th and 75th percentiles. (b) Temporal trend in the proportion of the area experiencing soil droughts from 1982 to 2016. (c) Spatial distribution of Pearson correlation coefficients between yield anomalies and the total number of drought days. (d) Pearson correlation coefficients between yield anomalies and the total number of drought days, with the light blue shading representing the 25th and 75th percentiles.

To account for seasonal variability, we converted daily SM data into weekly averages and computed percentile ranks based on weekly data from 1980 to 2018. Weekly SM values below the 20th percentile were classified as drought conditions, while values above this threshold were considered non-drought condition. A drought event was defined as starting when SM dropped below the 20th percentile and ending when it rose above this threshold during the maize-growing season. We focused on drought events with a minimum duration of 4 weeks (i.e., monthly droughts). Adjacent drought events were not merged in this study. It is worth noting that when the start time of the drought does not fall within the growing season, but the end time does, and the duration is 4 weeks or more, we capture such events and consider only the length of time within the growing period as the duration of this drought event. Meanwhile, the total number of drought days is defined as the cumulative duration of all drought events in the region for that year.

3. Results

3.1. Spatiotemporal Patterns and Changes in Soil Droughts and Maize Yields

Over the past three decades (1982–2016), the total number of soil drought days in China showed an increasing trend (Figure 1a), accompanied by a marked expansion in the spatial extent of soil drought occurrences (Figure 1b). Moreover, there are pronounced regional differences in the spatial patterns of both drought frequency and the total number of drought days (Figures S1a and S1b in Supporting Information S1), with both metrics tending to increase progressively toward the north. Since changes in soil moisture directly affect plant water availability and consequently plant productivity and crop yields (Wang et al., 2011), the worsening drought conditions are likely to have an increasingly negative impact on maize yields.

To evaluate the sustainability and stability of maize yield, this study employs two key indicators: the sustainability index of yield (SYI) (Singh et al., 1990), and the coefficient of variation (CV) (Tucker et al., 1991). A higher SYI indicates greater sustainability of the cropping system, while a lower CV reflects higher yield stability (Wang et al., 2023). Our results show that parts of the northeastern, northern, and much of southwestern China exhibit lower SYI values and higher CV values (Figures S1c and S1d in Supporting Information S1), indicating reduced sustainability and increased instability in maize yields across these regions. These patterns may be influenced by various factors, including climate change, technological development, policy shifts, and agricultural management practices. To isolate the effect of climate change, we used yield anomaly to represent changes in maize yield (See the "Methods" Section), thereby removing the influence of technological advancements, improved seed varieties, policy interventions, and other non-climatic factors.

Focusing solely on climate influence, we applied Pearson correlation analysis to examine the relationship between maize yield anomalies and soil drought. Figure 1c presents the spatial distribution of Pearson correlation coefficients between pixel-based yield anomalies and the total number of drought days across China. Regions with a significantly negative correlation (dark red pixels) account for 15% of the total area, while 55% of the area shows an insignificant negative correlation (pink pixels). The remaining 30% (gray pixels) fall into other categories, including positive or no correlation. Overall, a predominantly negative correlation between drought and yield anomalies is observed across most regions, with a significant negative correlation clustered notably is observed in northeastern and northern China. Furthermore, yield anomalies decrease significantly as the total number of drought days increases (Figure 1d). Negative yield anomalies indicate that actual yields are below expected levels, with smaller (more negative) values representing larger shortfalls. This demonstrates that yield anomalies tend to become more negative as the total number of drought days rises.

3.2. The Combined Impacts of Drought and Soil Salinity on Maize Yields

In addition to the direct impact of drought, soil salinity is a critical factor limiting agricultural production. Although maize is not typically cultivated in highly saline soils, previous studies indicate that drought can induce salt accumulation in soil, further hindering crop growth (Maas & Grattan, 1999; Perri et al., 2022). In the context of increasingly severe drought events, the co-occurrence of drought and soil salinity (CODS) subject plants to combined stress. To evaluate yield reductions from individual drought and CODS, we defined three conditions and analyed their corresponding yield anomalies. The first category is the normal condition, characterized by the absence of drought and saline soil. Saline soil is defined by excessive accumulation of soluble salts on the soil surface and in the root zone, with an electrical conductivity of the saturated soil extract (EC_e) ≥ 2 dS·m^{-1} (Abrol et al., 1988), a threshold marking the upper tolerance limit for salt-sensitive crops (Maas & Grattan, 1999). The second is the individual drought condition, characterized by the occurrence of drought and non-saline soil. The third is the CODS condition, involving the co-occurrence of drought and saline soil.

Our results reveal that CODS is associated with significantly more negative yield anomalies than individual drought, whereas normal conditions are associated with positive yield anomalies (Figure 2a and Figure S2 in Supporting Information S1). This indicates that negative maize yield anomalies are pronounced under drought stress and become even stronger under combined drought and salinity stress. In other words, the negative impact of CODS exceeds that of drought alone. These findings align with previous studies showing that salinity and drought exert additive negative effects on shoot and root biomass accumulation (Abdelraheem et al., 2019; Angon et al., 2022; Hanks et al., 1977; Ors et al., 2021). The interaction between the two stressors further intensifies their adverse effects, indicating that their combination amplifies the damage each causes individually (Angon et al., 2022; Sahin et al., 2018).

Furthermore, under drought conditions, yield anomalies continue to decline as salinity increases (Figure 2b and Figure S3 in Supporting Information S1). Previous studies have shown that yield decreases approximately linearly once salinity surpasses a crop-specific threshold (Hanks et al., 1977; Maas & Hoffman, 1977). Figure 2b shows that under drought, yield anomalies remain predominantly negative across all salinity levels, indicating that drought reduces yield independently of salinity. In contrast, without drought, yields show more varied responses to salinity (Figure S4 in Supporting Information S1). Specifically, when $EC_e \leq 1$ dS·m^{-1}, yield anomalies show a

10.1029/2026WR044233

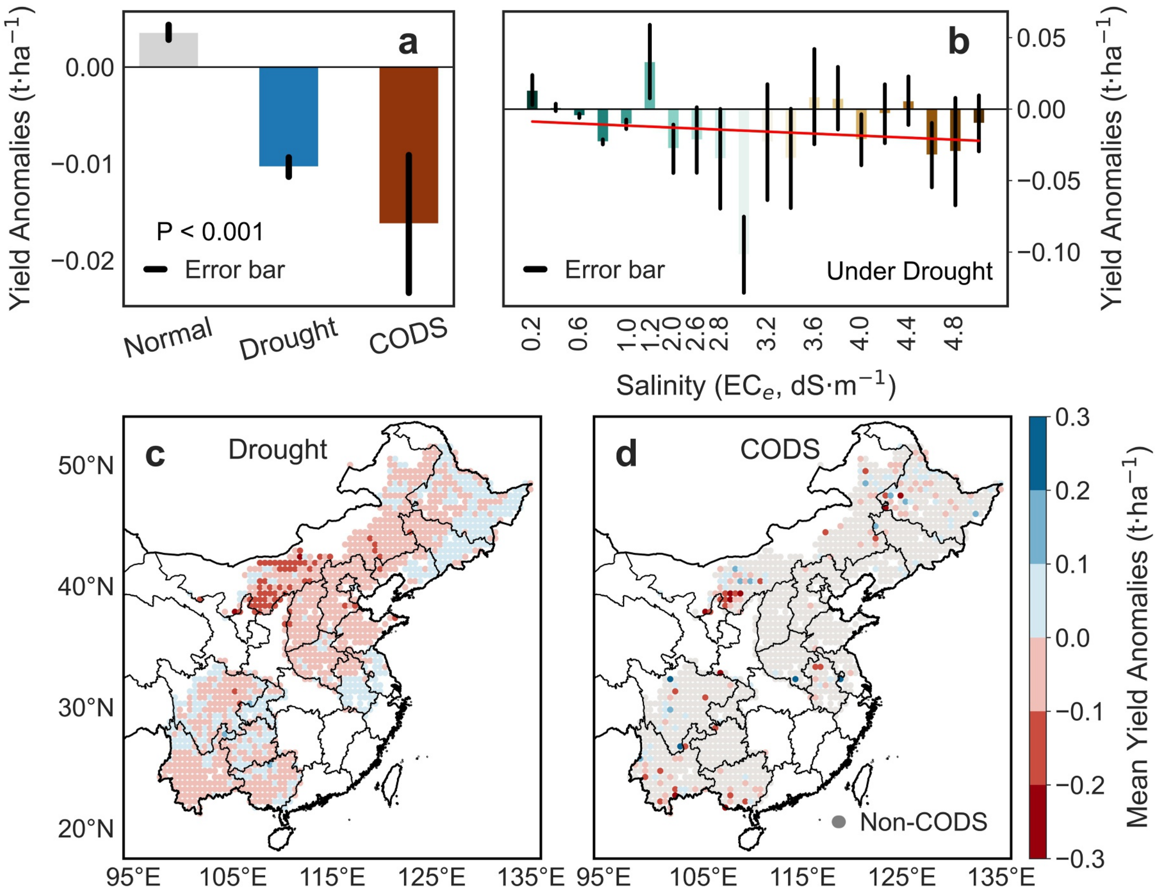

Figure 2. The effects of drought and salinity on maize yield. (a) Estimated effects of normal, individual drought, and CODS conditions on mean maize yield anomalies (t·ha^{-1}). (b) Estimated combined effects of drought and soil salinity under different salinity levels. Black line represents the error bars from 5% to 95% confidence interval. (c) Spatial distribution of the average effects of individual drought on maize yield from 1982 to 2016. (d) Spatial distribution of the average effects of CODS on maize yield from 1982 to 2016. Gray areas represent maize croplands where CODS events were not observed.

slight increasing tendency with rising EC_e. However, this pattern should not be interpreted as evidence of a direct physiological benefit of low salinity. At the gridded-field scale, it may partly reflect confounding effects associated with irrigation, fertile, or regional management practices. Therefore, we focus primarily on the negative yield responses observed under higher salinity levels and drought conditions. Figures 2c and 2d illustrate the spatial distribution of areas affected by individual drought and CODS, respectively. Drought affects nearly the entire study region, while CODS impacts are more localized.

To further evaluate maize yield loss in response to CODS, we estimated the risk of maize yield loss (defined as relative yield anomalies below −10%, or $y_t < -0.1$) using a copula-based model (See the "Methods" Section). Figure 3a shows the risk of yield loss under individual drought and CODS across China. Both conditions pose an approximately 20% risk of yield loss, though CODS presents a consistently higher risk than drought alone. Under combined stress, the risk of maize yield loss is approximately five percentage points higher than under drought stress alone. This risk also rises steadily with increasing salinity levels (Figure 3b). Across all salinity levels, the risk of yield loss under CODS remains about 5% higher than under individual drought. Under these varying salinity settings, CODS consistently showed a higher yield-loss risk than individual drought, and the estimated risk under CODS generally increased as the salinity threshold became more stringent. This result indicates that the amplifying effect of salinity on drought-related yield-loss risk is robust to the choice of ECe threshold. When salinity levels reach or exceed 5.0 dS·m^{-1}, the risk of yield loss under CODS surpasses 30%. Physiologically, drought limits the plant's access to available soil water, while the presence of salts during drought further increases osmotic stress and can induce ionic toxicity. These imbalances disrupt key physiological and biochemical pathways essential for growth and development (Zhang et al., 2013), indicating that salt stress effectively

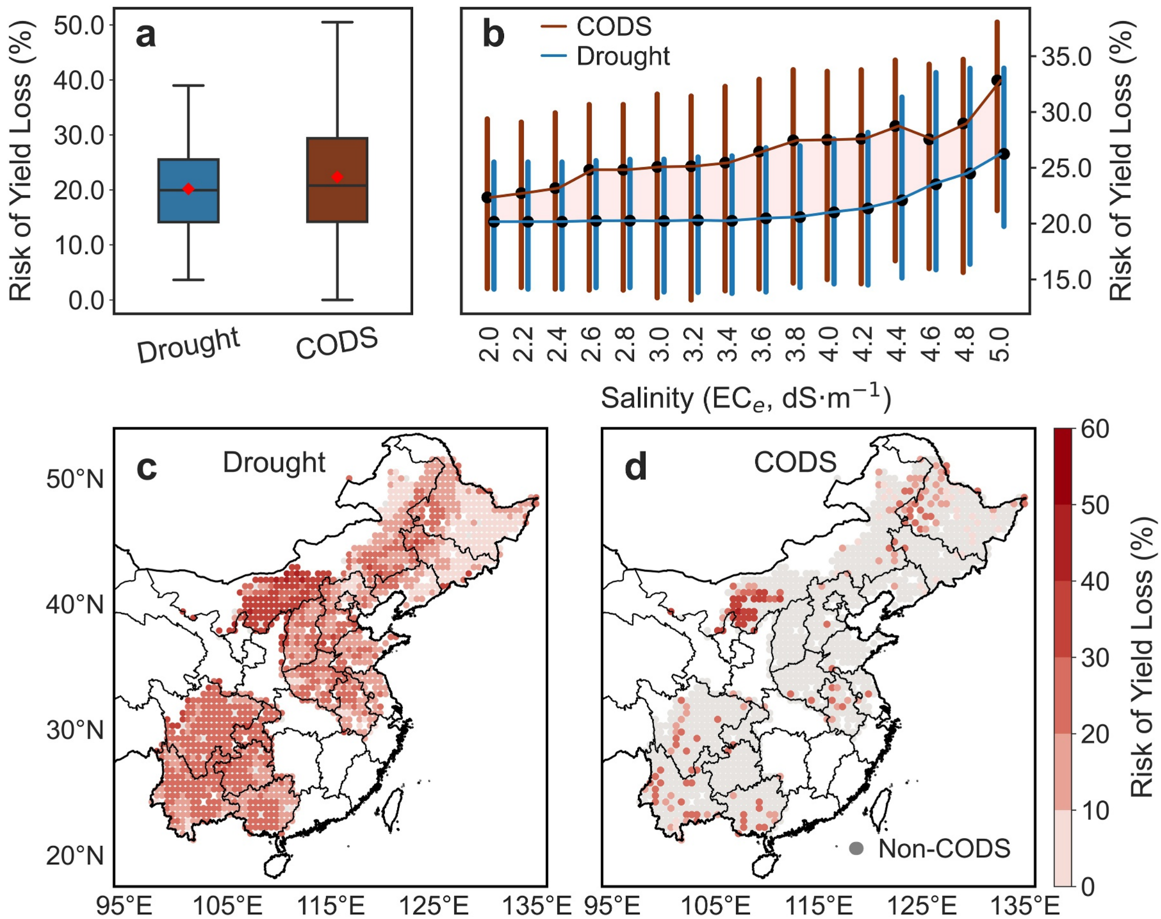

Figure 3. The risk of yield loss under individual drought and CODS. (a) The risk of yield loss under individual drought and CODS. The boxes represent the 25th and 75th percentiles. (b) Trend of yield loss risk under individual drought and CODS across different salinity levels. The *x*-axis represents a set of alternative ECe thresholds used to classify drought-affected samples into individual drought and CODS conditions. The black dot represents the mean value. The black solid line represents the 25th and 75th percentiles. (c) Spatial distribution of yield loss risk under individual drought. (d) Spatial distribution of yield loss risk under CODS. Gray areas represent the maize croplands where CODS events were not observed.

exacerbates drought stress (Rhoades et al., 1992). Spatially, the risk of yield loss under CODS is concentrated in northern China, particularly in the Songnen Plain, the southern North China Plain, and the northern Hetao Plain (Figures 3c and 3d).

We further validated the above conclusions using the GLEAM data set (Figure 4 and Figure S5 in Supporting Information S1) and the GlobalCropYield5min data set (Figure 5 and Figure S6 in Supporting Information S1), and obtained consistent results. These validation analyses provided consistent evidence for four main results, including the negative relationship between the total number of drought days and maize yield anomalies, the increasing trend in total number of drought days, the stronger negative effect of CODS on yield anomalies compared with individual drought, and the higher yield-loss risk under CODS than under individual drought. These results underscore impact variations in yield loss risk under individual drought and CODS, highlighting the stronger negativity of CODS on maize yield.

3.3. Attribution of Maize Yield Anomaly

Although the previous conclusions clearly demonstrate that CODS has a more severe negative impact on maize yield than drought alone, the influence of drought under CODS remains present, and the specific amplifying effect of salinity is not yet isolated. Furthermore, the key environmental drivers directly responsible for yield loss under CODS conditions remain unclear. To isolate the effects of drought variations, we first categorized the total number of drought days by month. Pixels with similar total drought durations, for example, 1 month, or more than

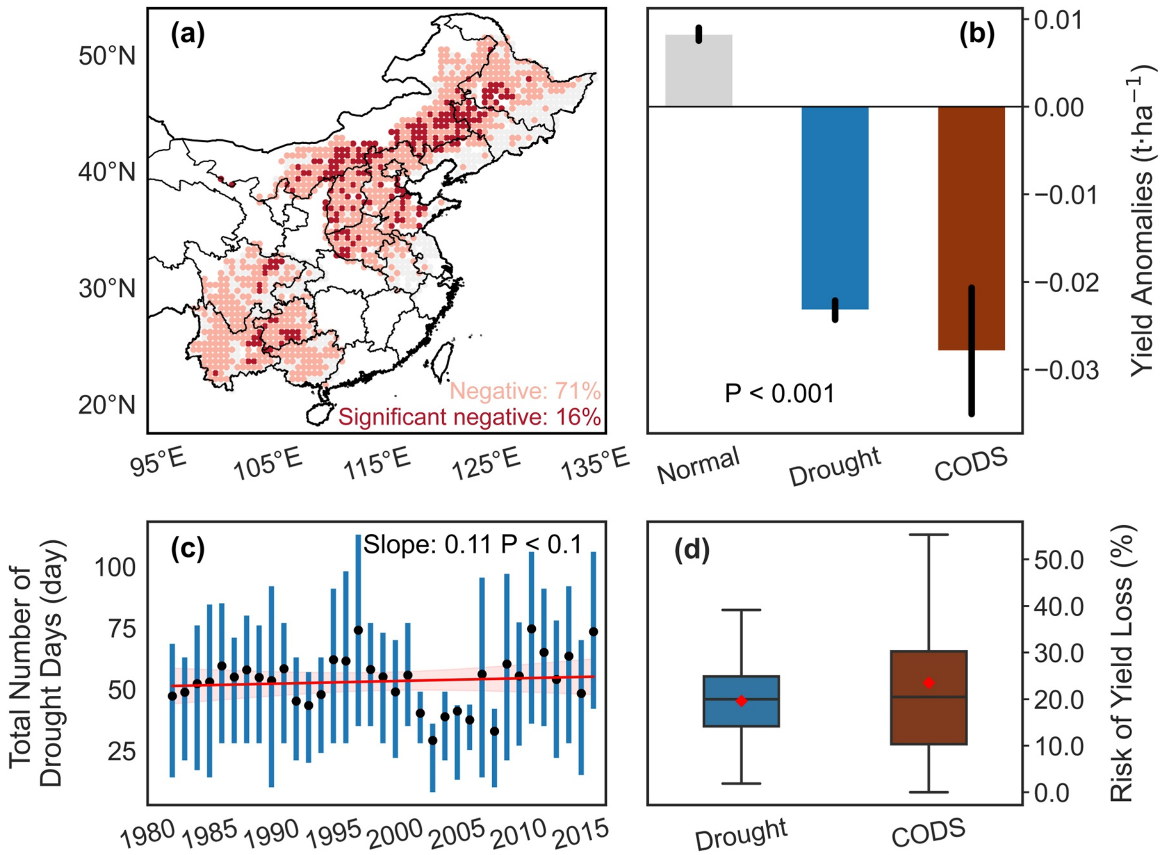

Figure 4. Validation of the core findings using the GDHY data and GLEAM data. (a) Spatial distribution of Pearson correlation coefficients between yield anomalies and the total number of drought days. (b) Estimated effects of normal, individual drought, and CODS conditions on relative maize yield anomalies (t·ha^{-1}). (c) Temporal trend in the total number of soil drought days from 1982 to 2016. The black dot represents the mean value. The blue solid line represents the 25th and 75th percentiles. (d) Risk of yield loss under CODS and individual drought. The boxes represent the 25th and 75th percentiles.

one but less than 2 months, were grouped together under the assumption of comparable drought stress. Within each drought category, we then compared yield anomalies between cases where salinity exceeded the threshold (CODS) and cases where it did not (individual drought). This analysis revealed more negative yield anomalies when salinity exceeded the threshold (Figure 6a). To further refine our control, we subdivided the soil moisture data within each monthly drought category into our percentile bins (0–25th, 25–50th, 50–75th, and 75–100th). By matching both the drought duration category and the soil moisture percentile, we created highly comparable drought conditions and obtained consistent results (Figure 6b). This suggests that, under similar drought stress, elevated salinity is associated with additional yield reduction.

To quantify the contribution of key factors to yield loss, we employed an XGBoost model and SHAP (Shapley Additive exPlanations) analysis (See the "Methods" Section). Given that severe soil droughts under global climate change are linked to anomalies in evapotranspiration, precipitation (P), and temperature (T) (Svoboda et al., 2002; Wang et al., 2011). We selected relevant climatic variables: T, VPD, potential evapotranspiration (PET), and P (Mukherjee et al., 2023; Nosetto et al., 2013), as along with EC_e for soil salinity. PET reflects atmospheric evaporative demand (Thornthwaite, 1948), while VPD dictates the evaporative demand on plant leaves (Jensen et al., 2016). Figure 6c shows that under individual drought conditions, drought-related variables (PET, P, SM, and VPD) contribute more to yield loss than salinity, consistent with established findings (Du et al., 2023; Sahin et al., 2018) and with drought being the primary stressor in this study. PET is the most important feature, with yield loss increasing as PET rises. In contrast, higher P and SM mitigated yield loss. Although EC_e has the smallest contribution, yield loss still worsens as EC_e increases. The overall model performance is good, with an AUC of 0.8056 and a Brier score of 0.1259. Under CODS conditions, drought-related variables still account for the largest share of contribution. However, the importance of salinity increased, ranking

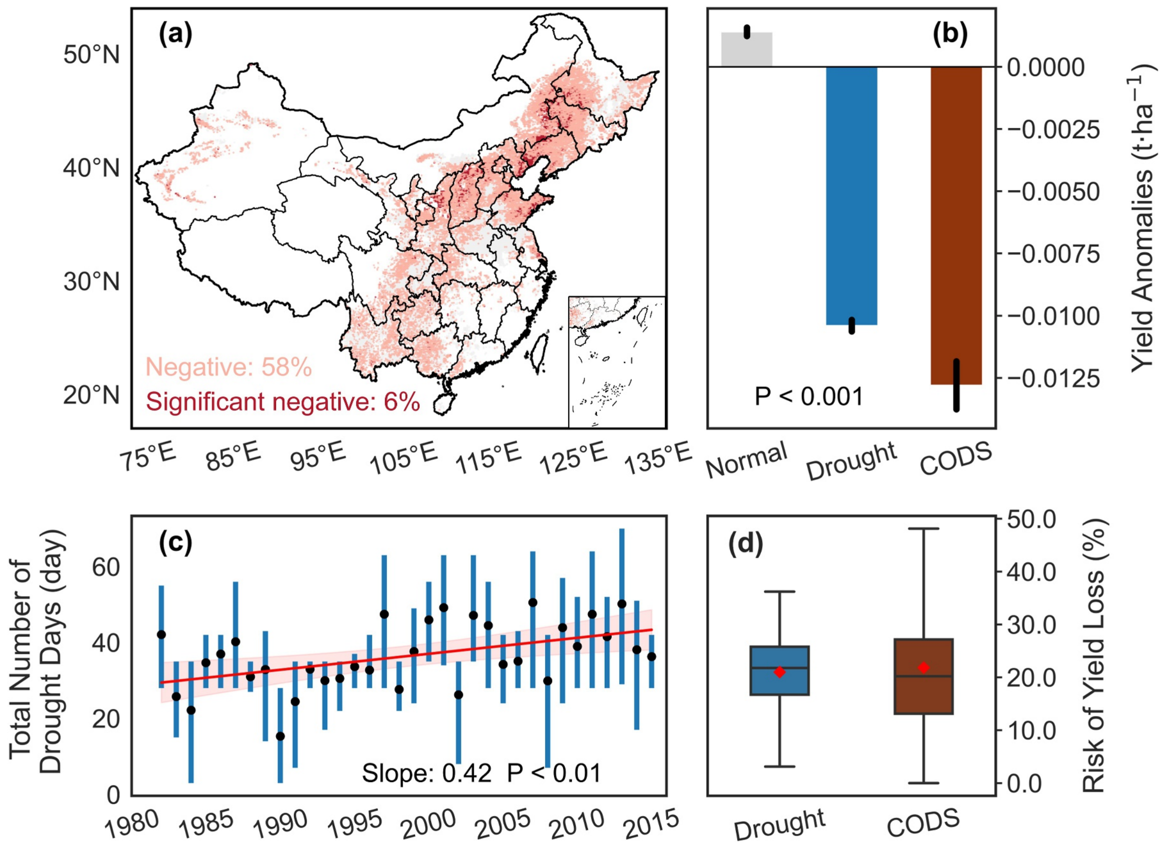

Figure 5. Validation of the core findings using GlobalCropYield5min data and ERA5 data. (a) Spatial distribution of Pearson correlation coefficients between yield anomalies and the total number of drought days. (b) Estimated effects of normal, individual drought, and CODS conditions on relative maize yield anomalies (t·ha^{-1}). (c) Temporal trend in the total number of soil drought days from 1982 to 2016. The black dot represents the mean value. The blue solid line represents the 25th and 75th percentiles. (d) Risk of yield loss under CODS and individual drought. The boxes represent the 25th and 75th percentiles.

just behind precipitation (Figure 6d). These results indicate that soil drought remains the dominant factor associated with maize yield loss, while the contribution of soil salinity becomes more pronounced under combined stress conditions.

3.4. Impact of Human Activities on Maize Yield

In this study, the impact of human activities on maize yield is considered primarily through increased soil salinity, which negatively affects crop productivity. Anthropogenic factors such as improper irrigation practices, the use of saline water for irrigation, and certain fertilization methods contribute directly or indirectly to the accumulation of salts in the soil (Corwin, 2021; Singh, 2015; Utset & Borroto, 2001). To better assess these effects, the study area was divided into rain-fed and irrigated regions using the Irrigated Area Map Asia 2010 for delineation. In rain-fed regions, salinity dynamics are driven by natural factors, whereas in irrigated regions, both natural and anthropogenic factors are involved. The Irrigated Area Map Asia 2010 was used to delineate rain-fed and irrigated zones (Siddiqui et al., 2016). An initial comparison between the two systems showed that soil salinity levels were significantly higher in irrigated regions than in rain-fed regions (Figure 7a). To isolate the influence of human activities, natural factors were simplified to drought conditions, with drought events categorized monthly. Pixels with similar total drought duration (e.g., 1 month, or more than one but less than 2 months) were grouped together under the assumption of comparable drought stress. Within each drought category, yield anomalies were compared for years with increasing versus decreasing soil salinity. Results reveal that increased salinity is associated with negative yield anomalies, indicating a decline in maize yield. Conversely, decreased salinity corresponds to positive anomalies, where actual maize yields exceeded expectations (Figure 7b). It is important to note that "increased salinity" here refers to an annual rise relative to the previous year, without applying a specific threshold.

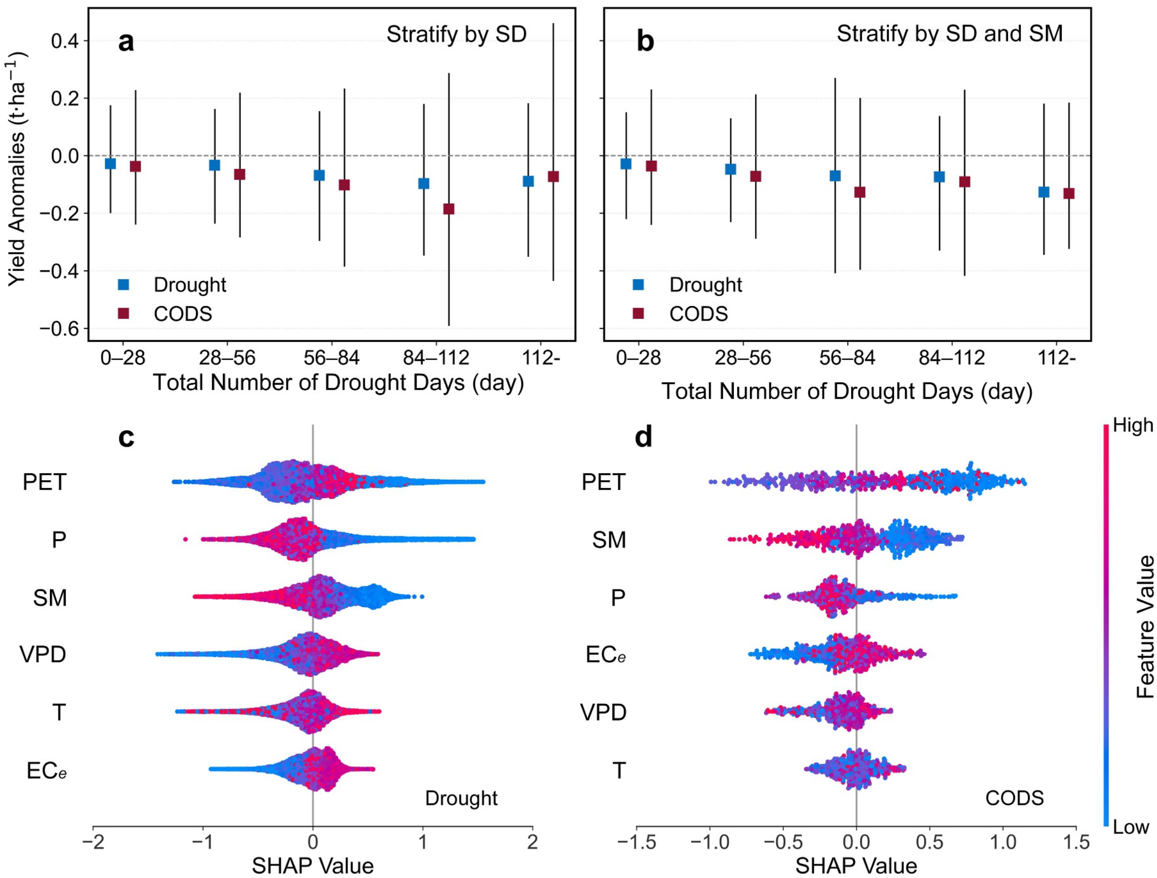

Figure 6. Feature importance analysis based on SHAP (Shapley Additive exPlanations) values. (a, b) Estimated effects of individual drought and CODS on relative maize yield anomalies under comparable drought stress (t·ha^{-1}). (a) Stratified by the total number of drought days. (b) Stratified by the total number of drought days and soil moisture. (c, d) SHAP summary plots showing the distribution of SHAP values across samples for each feature, colored by feature values from low (blue) to high (red). Features include PET, P, SM, Vapor pressure deficit, T, and EC_e. (c) Individual drought. (d) CODS.

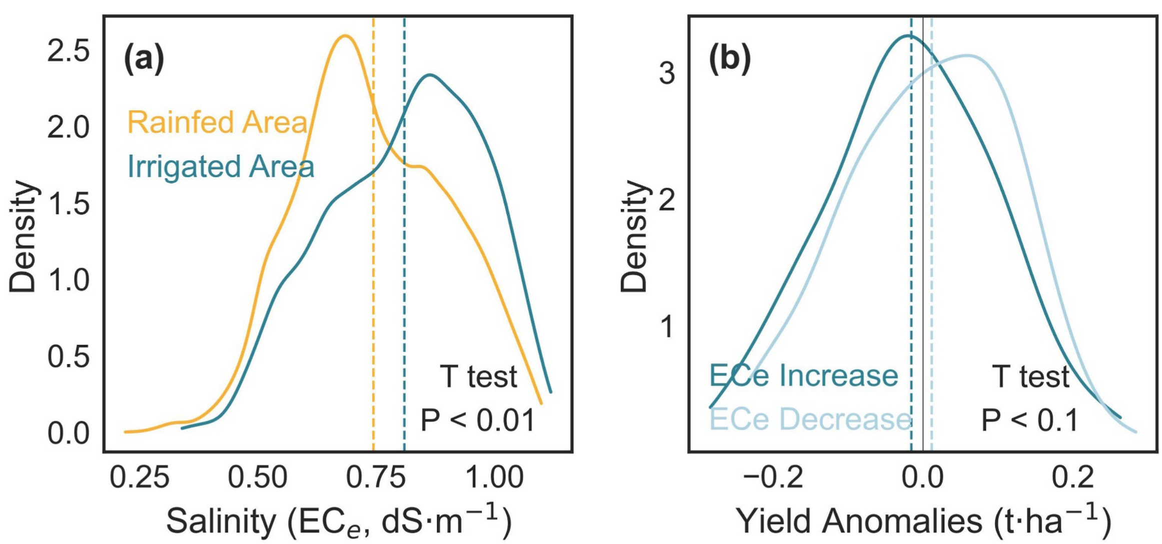

Figure 7. Density distribution of salinity level and maize yield anomalies under different conditions. (a) Comparison of salinity level between rain-fed area and irrigated area. (b) Comparison of maize yield anomalies between increased salinity and decreased salinity conditions.

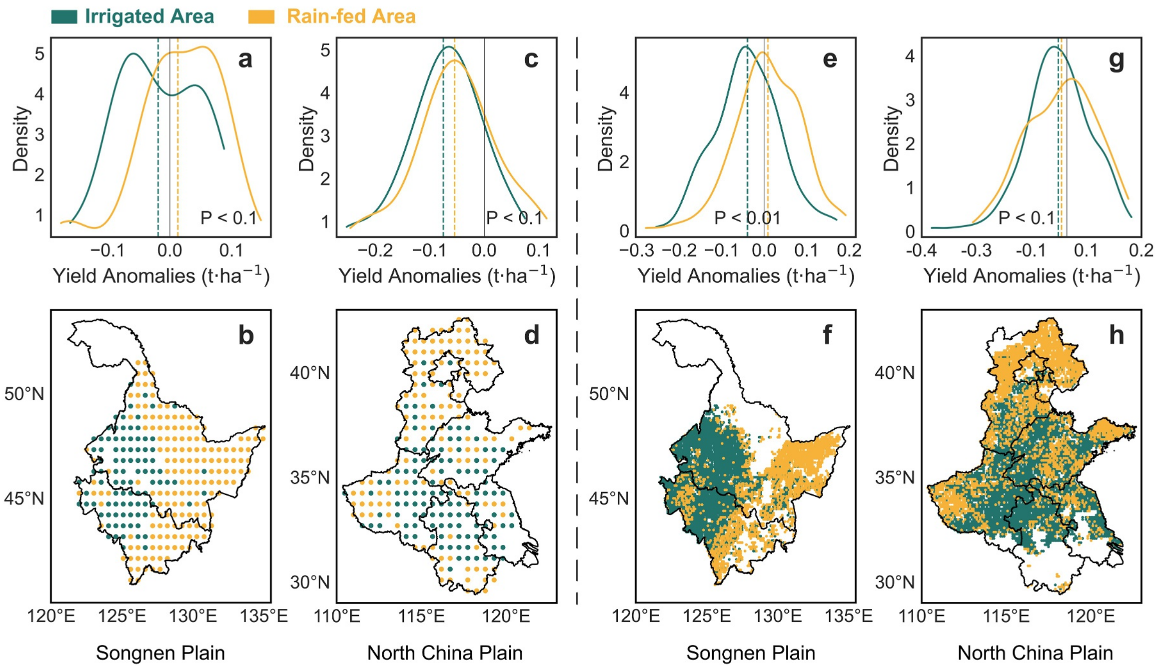

Figure 8. Density distribution of maize yield anomalies for irrigated and rain-fed areas in the Songnen Plain and the North China Plain. (a) Density distribution of maize yield anomalies for irrigated and rain-fed areas in the Songnen Plain (Global Data set of Historical Yields: GDHY data set). (b) Spatial distribution of irrigated and rain-fed grid cells in the Songnen Plain (GDHY data set). (c) Density distribution of maize yield anomalies for irrigated and rain-fed areas in the North China Plain (GDHY data set). (d) Spatial distribution of irrigated and rain-fed grid cells in the North China Plain (GDHY data set). (e) Density distribution of maize yield anomalies for irrigated and rain-fed areas in the Songnen Plain (GlobalCropYield5min data set). (f) Spatial distribution of irrigated and rain-fed grid cells in the Songnen Plain (GlobalCropYield5min data set). (g) Density distribution of maize yield anomalies for irrigated and rain-fed areas in the North China Plain (GlobalCropYield5min data set). (h) Spatial distribution of irrigated and rain-fed grid cells in the North China Plain (GlobalCropYield5min data set).

To further analyze the anthropogenic impact, we focused on two major maize-producing regions in China: the North China Plain and the Songnen Plain. These regions face similar challenges, including irrigation water shortages and salinity stress, and contains both rain-fed and irrigated systems under comparable natural conditions (Ben-Ari et al., 2018; Luo et al., 2018; Sun et al., 2010, 2006). Under equivalent drought conditions and periods of increasing salinity, irrigated areas exhibited more negative yield anomalies than rain-fed areas (Figures 8a and 8c). This indicates that additional salinity increase attributable to human activities leads to a more pronounced decline in maize yield. This conclusion is corroborated by an identical analysis using the higher-resolution (0.1°) GlobalCropYield5min data set (Figures 8e and 8g).

4. Discussions and Conclusions

This study examined the trends in maize yield in China from 1982 to 2016 against a backdrop of increasing soil drought. Our findings reveal an increasing trend in both the frequency and spatial extent of soil drought days. A significant negative correlation exists between soil drought and maize yield: as the total number of drought days increases, maize yield declines abnormally, particularly in northern and northeastern China. To assess the combined effects of soil drought and salinity, we compared the impacts of individual drought and CODS (co-occurrence of drought and soil salinity) during the maize-growing season. Both conditions reduce maize yield, but the negative trend is significantly more pronounced under CODS. A copula-based model further revealed that both individual drought and CODS pose approximately a 20% risk of yield loss, with CODS presenting a consistently higher risk. This risk escalates with rising salinity levels under both stress types, confirming that worsening salinity intensifies yield loss irrespective of drought conditions. In this study, CODS refers specifically to the co-occurrence of soil drought and soil salinity, the latter defined per FAO guidelines as having an electrical conductivity of the saturated paste extract (EC_e) ≥ 2 dS·m^{-1} (Abrol et al., 1988). While some studies suggest a maize salt tolerance threshold near $EC_e = 1.7$ dS·m^{-1} (Tanji et al., 2002). Our sensitivity analysis using three data combinations found no significant difference in yield anomalies between thresholds of 1.7 and 2 dS·m^{-1} (Figure S7 in Supporting Information S1). This is primarily due to the limited number of samples with soil salinity between these values across China (Figures S3 and S4 in Supporting Information S1). Consequently, a 2 $dS{\cdot}m^{-1}$ threshold was adopted.

By isolating drought variability, we confirmed that soil salinity exacerbates drought-induced yield loss under CODS. Using XGBoost and SHAP analysis, we quantified the contribution of key environmental variables, including VPD, PET, P, T, and EC_e, to yield loss. Under individual drought, drought-related variables (PET, P, and SM) were more influential than salinity (EC_e). However, the contribution of EC_e increased under CODS, highlighting salinity's amplifying role. To examine whether human activities may be linked to this process, we focused on the North China Plain and the Songnen Plain, two maize regions facing salt stress and saline irrigation. Under comparable drought conditions, irrigated areas, where salinity may be affected by irrigation-related practices, showed more negative yield anomalies than rain-fed areas. This suggests that salinity increases in irrigated areas, which may be partly influenced by human activities, are associated with more negative yield anomalies under comparable drought conditions.

Moving-window detrending may also partially remove low-frequency climatic variability and may be sensitive to endpoint treatment. To evaluate the sensitivity of the results to the detrending choice, we repeated the analysis using alternative 5-year and 9-year moving windows, as well as a centered moving window that excluded the focal year from the expected-yield calculation. The main conclusions remained consistent across these sensitivity analyses (Figures S9–S11 in Supporting Information S1), indicating that our findings are not driven by the choice of window length or the inclusion of the focal year.

A critical finding concerns the use of saline groundwater for irrigation in these freshwater-scarce regions. While this practice is viewed as an adaptive response to drought (Liu et al., 2024; Ma et al., 2008), our results suggest that if it leads to soil salt accumulation, it may ultimately undermine the goal of alleviating drought stress. EC_e increases with the concentration of irrigation water (Hagage et al., 2024; Han et al., 2024), and evaporative demand can simultaneously induce drought and salinity stress (Hailu & Mehari, 2021). Long-term saline water irrigation degrades soil structure (Panta et al., 2018), reduces key physiological parameters in maize like photosynthesis and transpiration (Wang et al., 2016), and leads to yield loss through salt accumulation (Baath et al., 2017). Even low-concentration saline water (<3 g/L) can cause significant yield losses over time (Wang et al., 2016). Therefore, water management strategies must consider both water quantity and quality to mitigate secondary salinization (Wen et al., 2022).

Sustainable saline water irrigation may require management practices that help control salt accumulation (Liu et al., 2024; Paranychianakis & Chartzoulakis, 2005; Wang et al., 2016), such as increased irrigation frequency, artificial drainage (Feng et al., 2021; Paranychianakis & Chartzoulakis, 2005), and adequate leaching to maintain long-term soil salinity within acceptable limits (Beltrán, 1999; Pasternak & De Malach, 1995). Although this study does not directly test specific irrigation interventions, our findings suggest that avoiding secondary salinization should be an important consideration in drought adaptation and irrigation management. This study underscores the significant risk that CODS poses to maize yield and provides evidence that unmanaged saline water use may exacerbate yield losses under drought conditions. Future research should prioritize these compound stresses to inform sustainable agricultural management and effective climate adaptation planning (Ibrahim et al., 2019; Ni et al., 2024).

One limitation of this study is that the EC_e data set used to represent soil salinity is based on machine-learning-derived estimates from remote sensing and environmental covariates, rather than direct field observations. Although this data set provides spatially continuous and long-term information on soil salinity, uncertainties may arise from model estimation, input data quality, and limited ground-based validation. Therefore, the salinity-related results should be interpreted as evidence based on gridded estimated salinity data, and future studies would benefit from direct field measurements to further validate these findings. Meanwhile, because this study is based on observational data sets and statistical model, our results should be interpreted as associations, conditional risk differences, and model-based feature contributions rather than direct causal estimates. Although the consistency across group comparisons, copula-derived conditional probabilities, validation data sets, and SHAP-based interpretation supports the robustness of the observed patterns, these approaches cannot fully exclude the influence of unobserved confounders, such as local irrigation timing and volume, fertilizer use, pest pressure, or other management practices. Therefore, the inferred amplifying role of soil salinity under drought should be interpreted cautiously. Future studies combining field experiments, process-based crop–soil models, and formal causal inference frameworks are needed to more rigorously quantify the causal contribution of soil salinity to drought-related maize yield losses. Furthermore, several data-related limitations should be acknowledged. First, the ERA5 soil moisture layers used in this study mainly represent shallow soil moisture conditions and may not fully capture deeper root-zone water availability for maize, particularly at later growth stages. Although the use of root zone soil moisture data from GLEAM at a depth of 0–100 cm as an independent validation data set produced consistent results, uncertainties related to dynamic soil moisture depth representation remain. In addition, the annual 0–30 cm EC_e product provides a long-term topsoil salinity indicator, but it cannot fully represent growing-season salinity dynamics or vertical salinity variation within the crop root zone. These limitations may introduce uncertainty into the estimated drought and salinity stresses. Nevertheless, the selected data sets provide spatially consistent, long-term information across China, making them useful for evaluating broad-scale associations between drought, salinity, and maize yield anomalies. Future studies would benefit from integrating depth-resolved root-zone soil moisture, seasonal salinity observations, and field-based measurements.

Conflict of Interest

The authors declare no conflicts of interest relevant to this study.

Availability Statement

All data sets used in this study are publicly available. The crop calendar data set (Sacks et al., 2010) is available at https://sage.nelson.wisc.edu/data-and-models/datasets/crop-calendar-dataset/. The Global Data set of Historical Yield (GDHY) (Iizumi & Sakai, 2020) for major maize and secondary maize yields is available at https://doi.pangaea.de/10.1594/PANGAEA.909132. The GlobalCropYield5min data set for maize yields is available at https://doi.org/10.17632/hg8wzgx4yp.3. The electrical conductivity of soil extract (EC_e) data set (Hassani et al., 2020) is available at https://doi.org/10.17632/v9mgbmtnf2.1. Soil moisture (SM) data set are provided by the European Centre for Medium-Range Weather Forecasts Reanalysis 5 (Hersbach et al., 2020) (ERA5, https://doi.org/10.24381/cds.e2161bac) and the Global Land Evaporation Amsterdam Model (Miralles et al., 2025) (GLEAM, https://doi.org/10.5281/zenodo.14724263). Climatic data sets (Harris et al., 2020) are provided by the gridded Climate Research Unit Time Series (CRU TS v.4.04, https://catalogue.ceda.ac.uk/uuid/89e1e34ec3554dc98594a5732622bce9). Relevant processed data of this study is stored at Zenodo (Li, 2026).

Acknowledgments
This study was supported by the Research Grants Council of the Hong Kong Special Administrative Region, China (Project No. PolyU/RGC 15232023) and the Hong Kong Polytechnic University (Project No. P0055919, P0060005).

References

Abdelraheem, A., Esmaeili, N., O'Connell, M., & Zhang, J. (2019). Progress and perspective on drought and salt stress tolerance in cotton. *Industrial Crops and Products*, *130*, 118–129. https://doi.org/10.1016/j.indcrop.2018.12.070

Abrol, I. P., Yadav, J. S. P., & Massoud, F. I. (1988). Salt affected soils and their management. *Food and Agriculture Organization of the United Nations*. https://www.fao.org/4/x5871e/x5871e00.htm

Andreadis, K. M., & Lettenmaier, D. P. (2006). Trends in 20th century drought over the continental United States. *Geophysical Research Letters*, *33*(10). https://doi.org/10.1029/2006GL025711

Angon, P. B., Tahjib-Ul-Arif, M., Samin, S. I., Habiba, U., Hossain, M. A., & Brestic, M. (2022). How do plants respond to combined drought and salinity stress? — A systematic review. *Plants*, *11*(21), 2884. https://doi.org/10.3390/plants11212884

Baath, G. S., Shukla, M. K., Bosland, P. W., Steiner, R. L., & Walker, S. J. (2017). Irrigation water salinity influences at various growth stages of Capsicum annuum. *Agricultural Water Management*, *179*, 246–253. https://doi.org/10.1016/j.agwat.2016.05.028

Beltrán, J. M. (1999). Irrigation with saline water: Benefits and environmental impact. *Agricultural Water Management*, *40*(2), 183–194. https://doi.org/10.1016/S0378-3774(98)00120-6

Ben-Ari, T., Boé, J., Ciais, P., Lecerf, R., Van Der Velde, M., & Makowski, D. (2018). Causes and implications of the unforeseen 2016 extreme yield loss in the breadbasket of France. *Nature Communications*, *9*(1), 1627. https://doi.org/10.1038/s41467-018-04087-x

Bentéjac, C., Csörgő, A., & Martínez-Muñoz, G. (2021). A comparative analysis of gradient boosting algorithms. *Artificial Intelligence Review*, *54*(3), 1937–1967. https://doi.org/10.1007/s10462-020-09896-5

Bhusal, N., Han, S.-G., & Yoon, T.-M. (2019). Impact of drought stress on photosynthetic response, leaf water potential, and stem sap flow in two cultivars of bi-leader apple trees (Malus × domestica Borkh.). *Scientia Horticulturae*, *246*, 535–543. https://doi.org/10.1016/j.scienta.2018.11.021

Cao, J., Zhang, Z., Luo, X., Luo, Y., Xu, J., Xie, J., et al. (2025). Mapping global yields of four major crops at 5-minute resolution from 1982 to 2015 using multi-source data and machine learning. *Scientific Data*, *12*(1), 357. https://doi.org/10.1038/s41597-025-04650-4

Challinor, A. J., Watson, J., Lobell, D. B., Howden, S. M., Smith, D. R., & Chhetri, N. (2014). A meta-analysis of crop yield under climate change and adaptation. *Nature Climate Change*, *4*(4), 287–291. https://doi.org/10.1038/nclimate2153

Chen, H., & Wang, S. (2023). Compound dry and wet extremes lead to an increased risk of rice yield loss. *Geophysical Research Letters*, *50*(24), e2023GL105817. https://doi.org/10.1029/2023GL105817

Chen, H., Wang, S., Zhu, P., & AghaKouchak, A. (2026). Winter wheat yield sensitivity to snow drought is increasing across the Northern Hemisphere. *Nature Food*, *7*(2), 174–184. https://doi.org/10.1038/s43016-026-01302-7

Chen, T., & Guestrin, C. (2016). XGBoost: A scalable tree boosting System. *Proceedings of the 22nd ACM SIGKDD International Conference on Knowledge Discovery and Data Mining*, 785–794. https://doi.org/10.1145/2939672.2939785

Corwin, D. L. (2021). Climate change impacts on soil salinity in agricultural areas. *European Journal of Soil Science*, *72*(2), 842–862. https://doi.org/10.1111/ejss.13010

Daryanto, S., Wang, L., & Jacinthe, P.-A. (2016). Global synthesis of drought effects on maize and wheat production. *PLoS One*, *11*(5), e0156362. https://doi.org/10.1371/journal.pone.0156362

Deb, P., Moradkhani, H., Han, X., Abbaszadeh, P., & Xu, L. (2022). Assessing irrigation mitigating drought impacts on crop yields with an integrated modeling framework. *Journal of Hydrology*, *609*, 127760. https://doi.org/10.1016/j.jhydrol.2022.127760

Dißmann, J., Brechmann, E. C., Czado, C., & Kurowicka, D. (2013). Selecting and estimating regular Vine copulae and application to financial returns. *Computational Statistics & Data Analysis*, *59*, 52–69. https://doi.org/10.1016/j.csda.2012.08.010

Du, Y., Liu, X., Zhang, L., & Zhou, W. (2023). Drip irrigation in agricultural saline-alkali land controls soil salinity and improves crop yield: Evidence from a global meta-analysis. *Science of The Total Environment*, *880*, 163226. https://doi.org/10.1016/j.scitotenv.2023.163226

Feng, G., Zhu, C., Wu, Q., Wang, C., Zhang, Z., Mwiya, R. M., & Zhang, L. (2021). Evaluating the impacts of saline water irrigation on soil water-salt and summer maize yield in subsurface drainage condition using coupled HYDRUS and EPIC model. *Agricultural Water Management*, *258*, 107175. https://doi.org/10.1016/j.agwat.2021.107175

Freedman, H., AghaKouchak, A., Rigden, A. J., Hoek, A., & Tomlinson, B. (2025). Disparities in the impact of drought on agriculture across countries. *Scientific Reports*, *15*(1), 13465. https://doi.org/10.1038/s41598-025-94166-z

Gebrechorkos, S. H., Sheffield, J., Vicente-Serrano, S. M., Funk, C., Miralles, D. G., Peng, J., et al. (2025). Warming accelerates global drought severity. *Nature*, *642*(8068), 628–635. https://doi.org/10.1038/s41586-025-09047-2

Ghaneei, P., Foroumandi, E., Stahl, K., Ajami, H., Wanders, N., & Moradkhani, H. (2026). Four decades of baseflow drought analysis reveals varying contributions of climatic drivers and physical controls. *Earth's Future*, *14*(1), e2025EF006934. https://doi.org/10.1029/2025EF006934

Hagage, M., Abdulaziz, A. M., Elbeih, S. F., & Hewaidy, A. G. A. (2024). Monitoring soil salinization and waterlogging in the northeastern Nile Delta linked to shallow saline groundwater and irrigation water quality. *Scientific Reports*, *14*(1), 27838. https://doi.org/10.1038/s41598-024-77954-x

Hailu, B., & Mehari, H. (2021). Impacts of soil Salinity/Sodicity on soil-water relations and plant growth in dry land areas: A review. *Journal of Natural Sciences Research*, *12*, 1–10.

Han, X., Li, D., Kang, Y., & Wan, S. (2024). Effect of saline water drip irrigation on tomato yield and quality in semi-humid area and arid area of China. *Irrigation Science*, *42*(2), 387–400. https://doi.org/10.1007/s00271-023-00870-x

Hanks, R. J., Sullivan, T. E., & Hunsaker, V. E. (1977). Corn and alfalfa production as influenced by irrigation and salinity. *Soil Science Society of America Journal*, *41*(3), 606–610. https://doi.org/10.2136/sssaj1977.03615995004100030036x

Harris, I., Osborn, T. J., Jones, P., & Lister, D. (2020). Version 4 of the CRU TS monthly high-resolution gridded multivariate climate dataset. *Scientific Data*, *7*(1), 109. https://doi.org/10.1038/s41597-020-0453-3

Hassani, A., Azapagic, A., & Shokri, N. (2020). Predicting long-term dynamics of soil salinity and sodicity on a global scale. *Proceedings of the National Academy of Sciences*, *117*(52), 33017–33027. https://doi.org/10.1073/pnas.2013771117

Hersbach, H., Bell, B., Berrisford, P., Hirahara, S., Horányi, A., Muñoz-Sabater, J., et al. (2020). The ERA5 global reanalysis. *Quarterly Journal of the Royal Meteorological Society*, *146*(730), 1999–2049. https://doi.org/10.1002/qj.3803

Hultgren, A., Carleton, T., Delgado, M., Gergel, D. R., Greenstone, M., Houser, T., et al. (2025). Impacts of climate change on global agriculture accounting for adaptation. *Nature*, *642*(8068), 644–652. https://doi.org/10.1038/s41586-025-09085-w

Hussain, M. I., Farooq, M., Muscolo, A., & Rehman, A. (2020). Crop diversification and saline water irrigation as potential strategies to save freshwater resources and reclamation of marginal soils—A review. *Environmental Science and Pollution Research*, *27*(23), 28695–28729. https://doi.org/10.1007/s11356-020-09111-6

Ibrahim, W., Qiu, C.-W., Zhang, C., Cao, F., Shuijin, Z., & Wu, F. (2019). Comparative physiological analysis in the tolerance to salinity and drought individual and combination in two cotton genotypes with contrasting salt tolerance. *Physiologia Plantarum*, *165*(2), 155–168. https://doi.org/10.1111/ppl.12791

Iizumi, T., & Sakai, T. (2020). The global dataset of historical yields for major crops 1981–2016. *Scientific Data*, *7*(1), 97. https://doi.org/10.1038/s41597-020-0433-7

Jensen, K. H., Berg-Sørensen, K., Bruus, H., Holbrook, N. M., Liesche, J., Schulz, A., et al. (2016). Sap flow and sugar transport in plants. *Reviews of Modern Physics*, *88*(3), 035007. https://doi.org/10.1103/RevModPhys.88.035007

Li, H. (2026). Soil salinity exacerbates the negative impact of drought on maize yields [Dataset]. *Zenodo*. https://doi.org/10.5281/zenodo.19087840

Li, Y., Wang, X., Xing, G., & Wang, D. (2024). Meteorological disaster disturbances on the main crops in the north–south transitional zone of China. *Scientific Reports*, *14*(1), 8846. https://doi.org/10.1038/s41598-024-59106-3

Li, H. (2025). Growing risk of soil salinization linked to soil droughts in a changing climate [Dataset]. *Zenodo*. https://doi.org/10.5281/zenodo.17433655

Liu, Z., Gao, C., Yan, Z., Shao, L., Chen, S., Niu, J., & Zhang, X. (2024). Effects of long-term saline water irrigation on soil salinity and crop production of winter wheat-maize cropping system in the North China Plain: A case study. *Agricultural Water Management*, *303*, 109060. https://doi.org/10.1016/j.agwat.2024.109060

Lobell, D. B., Roberts, M. J., Schlenker, W., Braun, N., Little, B. B., Rejesus, R. M., & Hammer, G. L. (2014). Greater sensitivity to drought accompanies maize yield increase in the U.S. midwest. *Science*, *344*(6183), 516–519. https://doi.org/10.1126/science.1251423

Lundberg, S. M., Erion, G., Chen, H., DeGrave, A., Prutkin, J. M., Nair, B., et al. (2020). From local explanations to global understanding with explainable AI for trees. *Nature Machine Intelligence*, *2*(1), 56–67. https://doi.org/10.1038/s42256-019-0138-9

Lundberg, S. M., & Lee, S.-I. (2017). A unified approach to interpreting model predictions. *Advances in Neural Information Processing Systems*, *30*. https://proceedings.neurips.cc/paper/2017/hash/8a20a8621978632d76c43dfd28b67767-Abstract.html

Luo, J., Shen, Y., Qi, Y., Zhang, Y., & Xiao, D. (2018). Evaluating water conservation effects due to cropping system optimization on the beijing-tianjin-hebei plain, China. *Agricultural Systems*, *159*, 32–41. https://doi.org/10.1016/j.agsy.2017.10.002

Ma, W., Mao, Z., Yu, Z., Van Mensvoort, M. E. F., & Driessen, P. M. (2008). Effects of saline water irrigation on soil salinity and yield of winter wheat–maize in North China Plain. *Irrigation and Drainage Systems*, *22*(1), 3–18. https://doi.org/10.1007/s10795-007-9027-1

Maas, E., & Grattan, S. (1999). Crop yields as affected by salinity. *Agricultural Drainage. Agron. Monograph*, *38*, 55–108.

Maas, E. V., & Hoffman, G. J. (1977). Crop salt tolerance—Current assessment. *Journal of the Irrigation and Drainage Division*, *103*(2), 115–134. https://doi.org/10.1061/JRCEA4.0001137

Mehrabi, Z., Delzeit, R., Ignaciuk, A., Levers, C., Braich, G., Bajaj, K., et al. (2022). Research priorities for global food security under extreme events. *One Earth*, *5*(7), 756–766. https://doi.org/10.1016/j.oneear.2022.06.008

Miralles, D. G., Bonte, O., Koppa, A., Baez-Villanueva, O. M., Tronquo, E., Zhong, F., et al. (2025). GLEAM4: Global land evaporation and soil moisture dataset at 0.1° resolution from 1980 to near present. *Scientific Data*, *12*(1), 416. https://doi.org/10.1038/s41597-025-04610-y

Mukherjee, S., Mishra, A. K., Zscheischler, J., & Entekhabi, D. (2023). Interaction between dry and hot extremes at a global scale using a cascade modeling framework. *Nature Communications*, *14*(1), 277. https://doi.org/10.1038/s41467-022-35748-7

National Bureau of Statistics of China. (2024). *China Statistical Yearbook 2024*. China Statistics Press. Retrieved from https://www.stats.gov.cn/sj/ndsj/2024/indexeh.htm

Ni, Y., Zhang, Q., Li, W., Cao, L., Feng, R., Zhao, Z., & Zhao, X. (2024). Selection and validation of reference genes for normalization of gene expression in Floccularia luteovirens. *Fungal Biology*, *128*(1), 1596–1606. https://doi.org/10.1016/j.funbio.2023.12.005

Nosetto, M. D., Acosta, A. M., Jayawickreme, D. H., Ballesteros, S. I., Jackson, R. B., & Jobbágy, E. G. (2013). Land-use and topography shape soil and groundwater salinity in central Argentina. *Agricultural Water Management*, *129*, 120–129. https://doi.org/10.1016/j.agwat.2013.07.017

Ors, S., Ekinci, M., Yildirim, E., Sahin, U., Turan, M., & Dursun, A. (2021). Interactive effects of salinity and drought stress on photosynthetic characteristics and physiology of tomato (Lycopersicon esculentum L.) seedlings. *South African Journal of Botany*, *137*, 335–339. https://doi.org/10.1016/j.sajb.2020.10.031

Ouyang, W., Struik, P. C., Yin, X., & Yang, J. (2017). Stomatal conductance, mesophyll conductance, and transpiration efficiency in relation to leaf anatomy in rice and wheat genotypes under drought. *Journal of Experimental Botany*, *68*(18), 5191–5205. https://doi.org/10.1093/jxb/erx314

Panta, S., Doyle, R., Hardie, M., Lane, P., Flowers, T., Haros, G., & Shabala, S. (2018). Can highly saline irrigation water improve sodicity and alkalinity in sodic clayey subsoils? *Journal of Soils and Sediments*, *18*(11), 3290–3302. https://doi.org/10.1007/s11368-018-1986-3

Paranychianakis, N. V., & Chartzoulakis, K. S. (2005). Irrigation of Mediterranean crops with saline water: From physiology to management practices. *Agriculture, Ecosystems & Environment*, *106*(2), 171–187. https://doi.org/10.1016/j.agee.2004.10.006

Pasternak, D., & De Malach, Y. (1995). Irrigation with brackish water under desert conditions X. Irrigation management of tomatoes (Lycopersicon esculentum Mills) on desert sand dunes. *Agricultural Water Management*, *28*(2), 121–132. https://doi.org/10.1016/0378-3774(95)01171-E

Perri, S., Molini, A., Hedin, L. O., & Porporato, A. (2022). Contrasting effects of aridity and seasonality on global salinization. *Nature Geoscience*, *15*(5), 375–381. https://doi.org/10.1038/s41561-022-00931-4

Rhoades, J. D., Kandiah, A., & Mashali, A. M. (1992). The use of saline waters for crop production. *Food and Agriculture Organization of the United Nations*.

Sacks, W. J., Deryng, D., Foley, J. A., & Ramankutty, N. (2010). Crop planting dates: An analysis of global patterns. *Global Ecology and Biogeography*, *19*(5), 607–620. https://doi.org/10.1111/j.1466-8238.2010.00551.x

Sahin, U., Ekinci, M., Ors, S., Turan, M., Yildiz, S., & Yildirim, E. (2018). Effects of individual and combined effects of salinity and drought on physiological, nutritional and biochemical properties of cabbage (Brassica oleracea var. Capitata). *Scientia Horticulturae*, *240*, 196–204. https://doi.org/10.1016/j.scienta.2018.06.016

Siddiqui, S., Cai, X., & Chandrasekharan, K. (2016). *Irrigated Area Map Asia and Africa*. International Water Management Institute. Retrieved from https://waterdata.iwmi.org/applications/irri_area/

Singh, A. (2015). Soil salinization and waterlogging: A threat to environment and agricultural sustainability. *Ecological Indicators*, *57*, 128–130. https://doi.org/10.1016/j.ecolind.2015.04.027

Singh, R. P., Das, S. K., Rao, V. M., & Reddy, M. (1990). Towards sustainable dryland Agricultural Practices. *Tech. Bull*, 1–106.

Soni, P. G., Basak, N., Rai, A. K., Sundha, P., Narjary, B., Kumar, P., et al. (2021). Deficit saline water irrigation under reduced tillage and residue mulch improves soil health in sorghum-wheat cropping system in semi-arid region. *Scientific Reports*, *11*(1), 1880. https://doi.org/10.1038/s41598-020-80364-4

Sun, H., Shen, Y., Yu, Q., Flerchinger, G. N., Zhang, Y., Liu, C., & Zhang, X. (2010). Effect of precipitation change on water balance and WUE of the winter wheat–summer maize rotation in the North China Plain. *Agricultural Water Management*, *97*(8), 1139–1145. https://doi.org/10.1016/j.agwat.2009.06.004

Sun, H.-Y., Liu, C.-M., Zhang, X.-Y., Shen, Y.-J., & Zhang, Y.-Q. (2006). Effects of irrigation on water balance, yield and WUE of winter wheat in the North China Plain. *Agricultural Water Management*, *85*(1), 211–218. https://doi.org/10.1016/j.agwat.2006.04.008

Svoboda, M., LeComte, D., Hayes, M., Heim, R., Gleason, K., Angel, J., et al. (2002). The drought monitor. https://journals.ametsoc.org/view/journals/bams/83/8/1520-0477-83_8_1181.xml

Tang, T., Ge, J., Shi, H., Wang, L., Cao, J., & Lee, X. (2025). Drought frequency, intensity, and exposure have increased due to historical land use and land cover changes. *Communications Earth & Environment*, *6*(1), 398. https://doi.org/10.1038/s43247-025-02392-0

Tanji, K. K., & Kielen, N. C., & with Food and Agriculture Organization of the United Nations). (2002). Agricultural drainage water management in arid and semi-arid areas. *Food and Agriculture Organization of the United Nations*. https://doi.org/10.5555/20033060122

The State of Food Security and Nutrition in the World 2020. (2020). The State of food security and nutrition in the world 2020. FAO, IFAD, UNICEF, WFP and WHO Retrieved from http://www.fao.org/documents/card/en/c/ca9692en

Thornthwaite, C. W. (1948). An approach toward a rational classification of climate. *Geographical Review*, *38*(1), 55–94. https://doi.org/10.2307/210739

Troy, T. J., Kipgen, C., & Pal, I. (2015). The impact of climate extremes and irrigation on US crop yields. *Environmental Research Letters*, *10*(5), 054013. https://doi.org/10.1088/1748-9326/10/5/054013

Tucker, C. J., Newcomb, W. W., Los, S. O., & Prince, S. D. (1991). Mean and inter-year variation of growing-season normalized difference vegetation index for the Sahel 1981-1989. *International Journal of Remote Sensing*, *12*(6), 1133–1135. https://doi.org/10.1080/01431169108929717

Utset, A., & Borroto, M. (2001). A modeling-GIS approach for assessing irrigation effects on soil salinisation under global warming conditions. *Agricultural Water Management*, *50*(1), 53–63. https://doi.org/10.1016/S0378-3774(01)00090-7

Wang, A., Lettenmaier, D. P., & Sheffield, J. (2011). Soil moisture drought in China, 1950–2006. *Journal of Climate*, *24*(13), 3257–3271. https://doi.org/10.1175/2011JCLI3733.1

Wang, A., Li, K. Y., & Lettenmaier, D. P. (2008). Integration of the variable infiltration capacity model soil hydrology scheme into the community land model. *Journal of Geophysical Research*, *113*(D9), 2007JD009246. https://doi.org/10.1029/2007JD009246

Wang, H., Zheng, C., Ning, S., Cao, C., Li, K., Dang, H., et al. (2023). Impacts of long-term saline water irrigation on soil properties and crop yields under maize-wheat crop rotation. *Agricultural Water Management*, *286*, 108383. https://doi.org/10.1016/j.agwat.2023.108383

Wang, Q., Huo, Z., Zhang, L., Wang, J., & Zhao, Y. (2016). Impact of saline water irrigation on water use efficiency and soil salt accumulation for spring maize in arid regions of China. *Agricultural Water Management*, *163*, 125–138. https://doi.org/10.1016/j.agwat.2015.09.012

Wen, W., Timmermans, J., Chen, Q., & van Bodegom, P. M. (2022). Monitoring the combined effects of drought and salinity stress on crops using remote sensing in the Netherlands. *Hydrology and Earth System Sciences*, *26*(17), 4537–4552. https://doi.org/10.5194/hess-26-4537-2022

Wen, W., Timmermans, J., Chen, Q., & Van Bodegom, P. M. (2023). Evaluating crop-specific responses to salinity and drought stress from remote sensing. *International Journal of Applied Earth Observation and Geoinformation*, *122*, 103438. https://doi.org/10.1016/j.jag.2023.103438

Xu, F., Qu, Y., Bento, V. A., Song, H., Qiu, J., Qi, J., et al. (2024). Understanding climate change impacts on drought in China over the 21st century: A multi-model assessment from CMIP6. *npj Climate and Atmospheric Science*, *7*(1), 32. https://doi.org/10.1038/s41612-024-00578-5

Xu, Y., Lin, K., Hu, C., Chen, X., Zhang, J., Xiao, M., & Xu, C.-Y. (2024). Uncovering the dynamic drivers of floods through interpretable deep learning. *Earth's Future*, *12*(10), e2024EF004751. https://doi.org/10.1029/2024EF004751

Zhang, B., Wang, S., Moradkhani, H., Slater, L., & Liu, J. (2022). A Vine Copula-based ensemble projection of precipitation intensity–duration–frequency curves at sub-daily to multi-day time scales. *Water Resources Research*, *58*(11), e2022WR032658. https://doi.org/10.1029/2022WR032658

Zhang, B., Wang, S., & Slater, L. (2024). Anthropogenic climate change doubled the frequency of compound drought and heatwaves in low-income regions. *Communications Earth & Environment*, *5*(1), 715. https://doi.org/10.1038/s43247-024-01894-7

Zhang, S., Wu, Y., Sivakumar, B., Mu, X., Zhao, F., Sun, P., et al. (2019). Climate change-induced drought evolution over the past 50 years in the southern Chinese Loess Plateau. *Environmental Modelling & Software*, *122*, 104519. https://doi.org/10.1016/j.envsoft.2019.104519

Zhang, Y., Zhang, F., Li, X., Baller, J. A., Qi, Y., Starker, C. G., et al. (2013). Transcription activator-like effector nucleases enable efficient plant genome engineering. *Plant Physiology*, *161*(1), 20–27. https://doi.org/10.1104/pp.112.205179

Zhou, S., Yu, B., & Zhang, Y. (2023). Global concurrent climate extremes exacerbated by anthropogenic climate change. *Science Advances*, *9*(10), eabo1638. https://doi.org/10.1126/sciadv.abo1638